Experimental Study on Fire Resistance of a Full-Scale Composite Floor Assembly in a Two-Story Steel Framed Building

Lisa Choe[1], Selvarajah Ramesh, Xu Dai, Matthew Hoehler, Matthew Bundy

National Institute of Standards and Technology, Gaithersburg, Maryland, USA

Abstract

The purpose of this paper is to report the first of four planned fire experiments on the 9.1 m × 6.1 m steel composite floor assembly as part of the two-story steel framed building constructed at the National Fire Research Laboratory. The fire experiment was aimed to quantify the fire resistance and behavior of full-scale steel-concrete composite floor systems commonly built in the United States. The test floor assembly, designed and constructed according to the 2-hour fire resistance rating, was tested to failure under a natural gas fueled compartment fire and simultaneously applied mechanical loads. Although the protected steel beams and girders achieved matching or superior performance compared to the prescribed limits of temperatures and displacements used in standard fire testing, the composite slab developed a central breach approximately at a half of the specified rating period. A minimum area of the shrinkage reinforcement (60 mm^2/m) currently permitted in the United States construction practice may be insufficient to maintain structural integrity of a full-scale composite floor system under the 2-hour standard fire exposure. This work was the first-of-kind fire experiment conducted in the United States to study the full system-level structural performance of a composite floor system subjected to compartment fire using natural gas as fuel to mimic a standard fire environment.

Key words

Composite floor; Steel structure; Fire resistance; Compartment fire; Large-scale fire testing

[1] Corresponding Author, lisa.choe@nist.gov

1. Introduction

1.1 Background

Steel-concrete composite floors have been used extensively in building construction because of their cost-effectiveness in spanning large open spaces. In the United States, fire safety design of composite floors is predominantly based on prescriptive fire-resistance requirements using the fire testing methods set forth in the ASTM E119 standard (ASTM, 2021). Standard fire testing is usually conducted on an isolated composite beam or floor assembly much smaller in size and with idealized support conditions due to the size limitations of furnaces. The testing method is strictly purposed to measure the thermal endurance of the specimens with passive fire protection details, such as a specific thickness of fireproofing materials applied to steel beams and that of concrete topping over profiled metal decking. The result from standard fire testing, namely, the *fire-resistance rating* of an individual building element, seldom provides technical basis for risk-informed design decisions to ensure the overall fire safety of a building.

Because of those inherent limitations in standard fire testing, there has been renewed interest in performance-based fire design as a result of tragic events in September 11, 2001. Some engineering methods have been developed along with guidance and design references, e.g., Appendix 4 of the AISC 360 Specification (AISC, 2016) and the ASCE Manual of Practice 138 (ASCE, 2018). Most of the resources relevant to composite floor construction, however, focus on either retained flexural strength of unrestrained composite beams at elevated temperatures or temperature-dependent material models used for advanced analyses. Significant knowledge gaps exist in understanding of failure mechanisms and integrity of composite floor systems under realistic fire exposure due to various sources of thermal restraints (e.g., long-span floor beams, beam-end connections, steel frame layouts, and slab continuity).

Some experimental research efforts were made in Europe to better understand the system-level performance of real-scale structures in fire (Bisby *et al*., 2013). Table 1 presents key features of previous large-scale fire tests on composite floor assemblies spanning an area larger than 50 m^2. The landmark research at Cardington (British Steel 1999; Wald *et al*., 2006) included a series of compartment fire tests performed in the eight-story steel-framed building. This test program used so-called *natural fire* created using wood cribs to mimic fuel loads of a typical office setting. The growth of a fire was highly influenced by the thermal boundary conditions of the compartment enclosures and opening schemes, resulting in the upper layer gas temperatures increasing slower than the Eurocode parametric curves. The compartment fire temperature reached the maximum range of 900 °C and 1100 °C, approximately 60 min to 100 min after ignition. On the other hand, both FRACOF (Zhao *et al.*, 2008) and COSSFIRE (Zhao and Roosefid, 2011) tests utilized furnace heating with the ISO 834 temperature-time relationship up to 2 hours.

The floor specimens in Table 1 consisted of concrete slabs cast in-situ on light gauge steel decking with a trapezoidal profile, acting compositely with steel beams (weighing 40 kg/m to 51 kg/m) via headed stud anchors. While the beam-to-column connections were flexible endplates, either fin plates or bolted double angles were used at the ends of the secondary beams. The steel deck flute used in those studies was approximately 60 mm deep, whereas the thickness of concrete toping (above the top flange of profiled decking) varied from 70 mm to 97 mm. Anti-crack steel mesh used in the Cardington tests was relevant to the British construction practice in 1990s, while the FRACOF and COSSFIRE tests used the larger area of steel mesh designed incorporating membrane action of composite slabs at elevated temperatures. Even though passive fire protection of the primary steel frames varied among the tests, the secondary beam was left unprotected during fire exposure.

All five experiments indicated that temperatures of the bare steel (secondary) beams reached nearly 1000 °C. The maximum vertical displacement of the heated floor assemblies was in the range of 27 cm to 120 cm, equivalent to the ratio of L/30 to L/8 where L is the length of the secondary beam(s). None of the test assemblies developed collapse mechanisms. The integrity of composite slabs was affected by splice failure of lapped steel mesh mats (e.g., Cardington Test 7 and FRACOF test). The Cardington tests demonstrated the ability of reinforced composite slabs to develop membrane action in fire and the possibility of eliminating fire protection of the secondary beams. This observation led to the development of a simplified analytical method (e.g., Bailey 2003) to predict the behaior of composite floor assemblies in membrane action at elevated temperatures. Both FRACOF and COSSFIRE projects further confirmed the benefit from membrane action using a larger amount of steel reinforcement in composite slabs to enhance their fire resistance under standard fire exposure. Those large-scale tests led to the development of a performance-based design tool of composite floor slabs for fire condition, such as MACS+ (Vassart *et al.*, 2014), which has been implemented in industry practice.

1.2 Research Motivation and Objectives

Transformation from prescriptive to performance-based fire design will require high-fidelity computational modelling to predict realistic fire exposure and responses of structures as a complete system. To date, a significant need exists for experimental data to guide validation of computational models that predict the structural fire performance of full-scale composite steel frames constructed following the United States standard practice. The large-scale tests mentioned above have provided useful insights into fire resilience of composite floor systems through membrane action at large displacements: however, the data and findings from those studies are more applicable to construction practice in Europe. In addition, none of those studies measured the actual heat energy (heat release rate) from test fires, essential for validation of computational fluid dynamics models used for performance-based fire design of structures. The National Institute of Standards and Technology (NIST) is therefore conducting a series of large-scale experiments to investigate the behavior and limit states of full-scale structural steel frames with composite floors exposed to compartment fires. This test program consists of two parts: In Phase 1, the structural fire performance of the 12.8 m long composite beams with simple shear connections was studied (Ramesh *et al*., 2019; Choe *et al*., 2019; Choe *et al*., 2020). Phase 2 study is currently in progress to conduct compartment fire tests on a full-scale two-story structural steel gravity frame with composite floors. Details of the experimental design and measurement systems are presented in Choe et al. (2021a).

This paper presents the first experiment of the Phase 2 study conducted at NIST's National Fire Research Laboratory (NFRL) (Bundy *et al*., 2016) on November 14, 2019. The fire test compartment was situated on the ground floor in the south-edge bay of the two-story prototype building. The 9.1 m by 6.1 m composite floor assembly was subjected to combined mechanical loads and a standard fire created using natural gas burners. The objective of this test was to measure the structural and thermal responses of the composite floor assembly designed and constructed following the current prescriptive approach in the USA and to evaluate its system-level fire resistance based on the ASTM E119 acceptance criteria. The experimental results presented herein will serve as baseline to compare with the results from the remaining experiments in the Phase 2 program and be used to guide the validation of computational models and design tools.

2. Test Structure

The two-story structural steel frame was constructed under the NFRL's 20 MW exhaust hood to conduct a series of single-bay compartment fire experiments; see Figure 1. The total height of the building was approximately 7.2 m. The steel frame consisted of three bays by two bays in plan with a total floor area of 18 m × 11 m, as shown in Figure 2. The composite floor slab was constructed on the entire first floor (3.8 m above the ground floor). The test floor assembly was situated in the south middle-edge bay on the first floor of the prototype building. The slab splices were utilized to conduct the remaining experiments in the same bay. The floor assembly within the slab splices will be reconstructed new for each test. On the second floor, the beam framing was erected only, with the same wide-flange steel shapes used for the first-floor framing. All steel columns were W12×106 shapes anchored to the laboratory strong floor. The four columns supporting the test floor assembly were spliced 92 cm above the concrete slab on the first floor, whereas the remaining columns were continuous over two stories.

2.1 Composite floor assembly

In the fire test bay, the 9.1 m long W16×31 beams were connected to the column flange or at midspan of the 6.1 m long W18×35 girder using standard shear tabs; see Figure 3(a). Extended shear tabs were used at the ends of W18×35 girders; see Figure 3(b). All other beams and girders were connected using bolted angles and extended shear tabs, respectively. All structural steel shapes and shear tabs were rolled from A992 steel (a minimum specified yield strength of 345 MPa) and A36 steel (a minimum specified yield strength of 250 MPa), respectively. The measured average yield strength of W16×31 and W18×35 shapes was (380 ± 40) MPa and (340 ± 5) MPa, respectively. The measured average yield and ultimate tensile strength of shear tabs was (290 ± 4) MPa and (440 ± 30) MPa, respectively.

The concrete slab was lightweight aggregate concrete (a minimum specified compressive strength of 28 MPa) cast on 76 mm deep formed steel decking. The concrete mixture included polypropylene fibers (2.4 kg/m^3) to mitigate thermally induced spalling as suggested by Maluk *et al*. (2017). A similar concrete mixture was used for the Phase 1 composite beam study (Ramesh *et al*., 2019). The concrete slab was cast approximately 5 months prior to fire testing. The moisture content of the concrete at time of fire testing was 7.6 % when measured according to ASTM C642 (ASTM, 2013). The compressive and splitting tensile strength measured one week after fire was (67 ± 3) MPa and (3.4 ± 0.4) MPa, respectively. As shown in Figure 3(c), the slab thickness was 83 mm required for the 2-hour fire resistance rating with the 76 mm deep exposed steel deck. The 3.4 mm diameter cold-formed welded wires, spaced 152 mm, was embedded 41 mm below the top surface of the concrete slab. The area of the steel reinforcement was 60 mm^2/m, equivalent to the minimum shrinkage reinforcement prescribed in the relevant U.S. design standard (SDI, 2017).

The concrete slab was acting partially composite with the steel beam frame through headed stud anchors (shaft Ø19 mm). For the W16×31 beams, a single headed stud anchor was welded on the top flange and the center-to-center spacing of studs was 305 mm. A pair of the same size stud anchors were welded atop the W18×35 girders at spacing of 356 mm, as shown in Figure 3(c). The degree of composite action was estimated at about 65 % of the ambient-temperature yield strength of the steel beams.

In addition, the 77 cm long, 180-degree hooked reinforcing bars (Ø13 mm) were placed perpendicular to the south edge beam in order to prevent separation of the heated concrete slab during the test. The slab splices were designed to mimic a continuous slab between the fire test bay and the surrounding bays. The construction detail at the northwest corner of the test bay is shown in Figure 4(a). As shown, the No. 4 reinforcing bars (Ø13 mm) extended from the surrounding bays were lapped with the welded wire reinforcement. The lap length was approximately 63 cm. Screw anchors mounted on the splice plates provided additional friction at the concrete-steel interface.

2.2 Fire compartment

Figure 4(b) shows a photograph of the fire test compartment, approximately 10 m long and 7 m wide. The height of the composite floor soffit was 377 cm above the compartment floor. The enclosing walls were constructed with 300 cm tall sheet steel metals and a 4.8 cm thick gypsum board liner (3 layers of 15.9 mm thick gypsum boards) on the exposed wall surface. The 80 cm gap between the compartment ceiling and the top edges of the three internal walls was lined with two layers of 25 mm thick ceramic blankets. Four natural gas burners (1.5 m × 1 m each) were distributed across the floor of the test compartment. The main opening was on the south wall, approximately 150 cm tall × 582 cm wide. There was a 30 cm tall × 582 cm wide slit on the north wall, designed for air intake only. The height of the windowsill was 100 cm above the laboratory strong floor.

The exposed steel frame within the test compartment, shown in Figure 2, was sprayed with a gypsum-based cementitious material (average specified density of 295 kg/m^3) for the 2-hour fire resistance rating. The average thickness of sprayed fireproofing was measured 18 mm for both primary W16×31 beams and W18×35 girders and 13 mm for the secondary W16×31 beam. The coefficient of variation in thickness measurements was approximately 15 %. The exposed steel connections and columns were over sprayed with the same fireproofing material, with the thickness ranging from 25 mm to 28 mm.

3. Fire Test Conditions

The total mechanical load imposed on the 9.1 m × 6.1 m test floor assembly was approximately 150 kN ± 1%, needed to meet the American Society of Civil Engineers (ASCE) gravity load combination (ASCE, 2016) of 1.2×dead load + 0.5×live load for extraordinary events. This load was distributed at twenty-four points across the test floor using water-cooled loading frames connected to four hydraulic actuators mounted in the basement, Figure 5. The total floor load including the assembly self-weight was approximately 5 kPa. The surrounding floors were loaded by the 51 cm diameter water-filled drums (weighing 2.1 kN each), simulating a uniformly distributed mechanical load about 1.3 kPa. The load ratio (i.e., total load normalized by the ambient design capacity) of the test assembly was approximately 0.3 for both the secondary composite beam and the standard shear tabs of the same beam. The load ratio of the steel members and connections in the surrounding bays was less than 0.2.

The hydraulically loaded test floor assembly was exposed to a natural gas fueled compartment fire, Figure 6(a), simulating the ASTM E119 time-temperature curve. Figure 6(b) shows the burner heat release rate (HRRburner) versus time relationship used in this test. This relationship was verified through a series of mock-up tests (Zhang *et al*., 2019) conducted prior to this experiment. It should be noted that, as shown in Figure 6(b), there was a short loss (< 3 min) of the HRRburner data at 102 min due to network disruption of the natural gas delivery system. The fire and mechanical loads were removed at approximately 107 min. The total expanded uncertainty in measurements of the burner heat release rate and mechanical load was estimated 1.4 % at 10 MW (Bryant and Bundy, 2019) and 1 % at 150 kN, respectively. This incorporated a coverage factor of 2 with a level of confidence of approximately 95 % as defined in Taylor and Kuyatt (1994).

4. Results and Observations

4.1 Thermal response

Over two-hundred type-K thermocouples (bead Ø 0.5 mm) were deployed at various locations across the test assembly. The average upper layer gas (ULG) temperature within the test compartment was measured using twelve Inconel-sheathed thermocouple probes hanging 305 mm below the exposed steel deck. The average ULG temperature exceeded 700 °C at 11 min and reached its peak value of 1060 °C at 107 min. After 15 min from the burner ignition, the increase in the average ULG temperature resembled the International Organization for Standardization (ISO) standard 834 (ISO, 2019) temperature and was about 5 % higher than the ASTM E119 temperature. The standard deviation of this temperature measurement was estimated less than 50 °C, indicating practically uniform temperatures below the test floor assembly.

Figure 7 illustrates a temperature rise in the composite beams compared to the evolution of the upper layer gas temperature within the test compartment. For the W16×31 composite beams, the web and bottom flange of the protected steel beams were heated to 600 °C on average at 60 min and to 800 °C at 107 min, Figure 7(a). The average concrete temperature above the steel beam, approximately 0.5 mm above the top rib of the steel decking, increased to 270 °C at 107 min. Temperatures of headed stud anchors and welded wire reinforcement (WWR) remained below 400 °C and 200 °C, respectively.

For the W18×35 composite girders, as shown in Figure 7(b), the lower portion of the protected steel girders was heated to 450 °C at 60 min and 700 °C at 107 min. The top flange steel temperature remained below 400 °C. The bottom concrete temperature in the shallow section next to the steel girder increased to 600 °C at 80 min but significantly influenced by combined effects of concrete fractures and debonding of steel decking afterwards. The average temperatures of headed studs (at 2.5 cm above the steel decking) and WWR placed above the girders never exceeded 300 °C and 200 °C, respectively, during and after fire exposure.

The standard deviation in measured temperatures of the three heated W16×31 beams ranged from 60 °C to 110 °C, as indicated by error bars in Figure 7(a). This temperature variation might be caused by thermally induced fissures and degradation in fireproofing materials as the beams were undergoing severe thermal elongation and bending under fire loading. Unlike W16×31 beams, one can observe a smaller temperature difference (30 °C to 60 °C) between the east and west W18×35 girders, Figure 7(b). These girders did not deform significantly and therefore the applied fireproofing appeared to maintain relatively good integrity during fire loading.

A total of thirty-six thermocouples were mounted on the 9.1 m by 6.1 m test floor slab at various locations that were not thermally shaded by the steel framing underneath. Figure 8 shows the average concrete temperature in the 159 mm thick or 83 mm thick sections of the concrete slab. Thermocouples installed at the steel decking (TST-5*) measured the hottest temperature, reaching nearly 900 °C during fire loading. The peak temperature of the concrete near the bottom rib of the steel decking (TST-4) was about 100 °C higher than the concrete temperature near the top rib (TST-7). However, the spatial temperature variation of TST-5* and TST-7 was quite high (> 110 °C), as indicated by the large error bars. These temperatures could be sensitive to separation of the steel decking from the concrete. Temperatures of the welded wire reinforcement were affected by varying thickness of the concrete slab. At 107 min, for example, TST-1 (at deep sections) and TST-6 (at shallow sections) was 120 °C and 380 °C, respectively. In addition, the concrete temperatures towards the top surface (TST-1, TST-5, and TST-6) or at the centroid of the deep section (TST-2) were affected by evaporative cooling of the moisture driven out to the top surface, as evidenced by the temperature plateau at 100 °C, over a longer period.

Although the data are not presented in this paper, the top (unexposed) surface temperature measured using eight randomly distributed thermocouples continued to rise during the cooling phase (up to 1 hour following extinguishment), reaching 140 °C to 180 °C. Temperatures of the beam-to-girder shear tabs reached over 600 °C, whereas those of the shear-tab connections to columns were below 400 °C due to a thicker insulation sprayed on those regions. Detailed discussions and results of the connection temperatures are presented in Dai *et al*. (2020). Estimates of total expanded uncertainty (with a coverage factor of 2) in measurements of the gas-phase, steel, and concrete temperatures are 8 % at 1110 °C, 6 % at 970 °C, and 8 % at 310 °C, respectively.

4.2 Structural response

The mechanically loaded test floor assembly continuously sagged during heating, while sequentially developing concrete fractures at various locations. No explosive spalling of the concrete was visible during or after the experiment, however, small 'popping' sounds continued during heating. This might indicate that (micro) spalling was occurring between the bottom of the slab and the steel deck. Concrete surface cracks first appeared along the east and west girders as well as the north edge beam of the test bay about 20 min to 30 min after ignition. Around 40 min into heating, the southeast corner of the heated floor slab fractured with a loud noise. After 70 min, tensile fracture of the concrete was visible near the longitudinal (east-west) centerline of the test floor. Reaching 100 min in fire, small flames were intermittently visible above the top of the heated slab towards the east and west ends of this longitudinal crack, indicating failures of some screw joints of steel deck units in those locations. From this point forward, the mechanical loads on the south side of the test slab appeared to be supported by the steel deck and the south edge beam with concrete hanging cantilever, Figure 9(a). The fire and mechanical loading were removed at 107 min due to safety concerns.

A total of thirty displacement transducers were deployed to measure the displacement of the two-story steel frame and the 9.1 m by 6.1 m test floor assembly during and after fire exposure. Figure 9(b) shows locations of the selected vertical and horizontal displacement sensors (labelled VD and HD, respectively) of the test assembly. All VD sensors in Figure 9(b) were located at the transverse (north-south) centerline of the test assembly. HD4 and HD6 sensors were used to measure thermal expansion at the perimeter of the heated floor assembly in the east-west direction and the north-south direction, respectively. HD9 measured the lateral displacement of the southeast column at the first story level. These horizontal displacement measurements were made at 15 cm above the top surface of the test floor slab. The total expanded uncertainty (with a coverage factor of 2) in measurements of the vertical and horizontal displacements is estimated 2 % at 580 mm and 6 % at 35 mm, respectively.

As shown in Figure 10, the vertical displacement of the test floor assembly continued to increase during heating and partly recovered during cooling; however, collapse did not occur. It is noteworthy that the actuator loads on the heated floor were removed immediately after the burners were switched off at 107 min, and therefore the test floor assembly supported the weight of loading frames (approx. 0.45 kPa) during the cooling phase. Until 60 min after ignition the values of VD5 and VD8 were similar. However, after the test floor slab began to breach (wide longitudinal crack) around 70 min, VD5 surpassed VD8 and reached 460 mm at 92 min. This displacement was approximately equal to the ratio of L/20 where L is the east-west span of 9.1 m. While VD5 finally reached the L/16 ratio at 107 min, there was no indication of 'runaway' deformation. Conversely, the vertical displacements of the perimeter steel members (VD1, VD7, VD10, and VD11) were relatively small, ranging from 65 mm to 210 mm. Also, VD7 and VD11 appeared to be less affected by the longitudinal concrete fractures. These perimeter members exhibited some degree of twisting and lateral deformations discovered during the post-test inspections.

Figure 11(a) shows the midspan vertical displacements of the protected steel beams and girders as a function of the bottom flange temperatures. When the bottom flange temperature exceeded 700 °C, the vertical displacement of the secondary beam (VD5) increased much more rapidly from 0.4 mm/°C to 1.4 mm/°C. This change could be caused by several factors, such as initiation of a longitudinal breach of the test floor slab and continuous degradation of flexural strength and stiffness of support beams at higher temperatures. In the early stage of a test fire, on the other hand, the increase in displacements of the east and west girders (VD7 and VD11, respectively) was affected by smaller applied load ratios than the secondary beam.

Furthermore, the heating rate of these members was relatively slow due to larger heat capacity and any heat loss associated with their close proximity to the upper wall lining with ceramic blankets or concrete fractures above these members. The vertical displacement of the south edge beam (VD10) was more responsive to the temperature change than other three perimeter members due to its free slab edge allowing less resistance to lateral-torsional buckling of this beam.

The horizontal (axial) displacements of the test assembly were measured using the lateral displacements of the columns at the first-story level. Figure 11(b) shows the time-varying horizontal displacement of the north primary beam (HD4) and the east girder (HD6) of the test assembly as well as the lateral displacement of the southeast column of the test bay. The positive values in this figure represent the displacements due to thermal expansion of the heated test assembly. The values of HD6 and HD9 were similar throughout the test, indicating that the east girder expanded in one direction, i.e., toward the south due to a much larger restraint provided by the north surrounding frame. These displacements increased continuously to a peak value ranging from 32 mm to 34 mm until the fire test was terminated. The value of HD4 increased at a similar rate but began to decrease after 70 min when the longitudinal fracture of concrete occurred. The maximum axial displacement due to thermal expansion in the east-west direction was approximately 22 mm.

Figure 12 shows the final fracture pattern of the test floor slab after cooling. As mentioned earlier, concrete cracks developed along the north, east, and west edges of the test bay, followed by the longitudinal cracks 530 mm or less south of the secondary beam. Most of welded wire reinforcement (60 mm^2/m) across the thicker lines of fractures visible in Figure 12 completely ruptured. Neither concrete failures along the south (free) edge (i.e., separation from the south edge beam) nor slab splice failures were witnessed. Based on crack openings of the concrete, the east and west edge cracks were initiated near the flanges of the southeast and southwest columns, whereas the north edge crack was propagated from the midspan or its vicinity. No through-depth fractures were observed around the northeast and northwest columns.

The middle breach of the test floor slab appeared to be occurred due to catenary action in the north-south direction where the steel decking was continuous into the north adjacent bay. It is believed that tensile membrane action was not achieved or developed in a limited fashion because of the early formation of concrete fractures and ruptures of welded wire reinforcement along the east and west edges. These through-depth cracks located 100 mm or less inside of the test-bay column grid, which formed shortly after fire ignition and continued to widen during heating. Hence, the headed stud anchors welded atop the east and west girders were ineffective to induce tension in the concrete in the east-west direction as the heated floor slab continued to deflect downward. In contrast, the north edge crack formed 370 mm or less north of the north primary beam (i.e., outside of the test-bay column grid) and thereby the headed stud anchors on all three 9.1 m long beams appeared to provide anchorage of the concrete and steel decking against tension developing in the north-south direction. As the vertical displacement of the test floor increased in fire, the excessive tension would develop more effectively in the north-south direction than in the east-west direction until welded wire reinforcement finally ruptured at critical locations. This welded wire reinforcement rupture would happen in the concrete where the vertical displacements were greater, i.e., south of the secondary beam (VD8) as shown in Figure 10(b).

Figure 13 shows the underside of the test floor assembly after cooling. The steel deck below concrete fractures (Figure 12) mostly maintained its integrity with good ductility. Only a local rupture was found in some deck units below the east end of the mid-panel longitudinal crack, i.e., near the west edge of the top flange of the east girder. All three 9.1 m long W16×31 beams exhibited permanent strong axis bending deformation and local buckling toward the beam ends. Furthermore, the north and south primary beams also exhibited twisting and lateral deformation. Although the north beam developed local buckling toward its ends, the shear tabs of the north and south beams maintained structural integrity. The east and west W18×35 girders showed little residual vertical deflection and exhibited minor out-of-plane deformations in the webs near the end connections. The extended shear tabs welded to the northeast and the northwest column webs exhibited noticeable out-of-plane deflection but no bolt failures. The extended shear tabs welded to the southeast and the southwest column webs deflected little, but the lower bolts of the southeast connection were partially ruptured in shear. The fireproofing sprayed on the beams and girders mostly remained intact, although fissures were evident on the beam web near the end connections and at the lower beam web of the secondary beam at midspan.

5. Comparison with ASTM E119 criteria

The intent of standard fire-resistance testing, mostly performed using a purpose-built furnace, is to provide a consensus-based method to evaluate the duration for which an isolated floor assembly contains a fire while retaining its structural stability, the so-called fire resistance rating expressed in minutes or hours. This testing is typically performed using a test assembly with limited size, e.g., a minimum floor area of 16.7 m^2 and a minimum beam span of 3.7 m

(ASTM, 2019) with two possible end support conditions; either restrained or unrestrained. While subjected to standard furnace heating, mechanical loads ranging from 50 % to 70 % of the ambient design capacity estimated for normal conditions (e.g., 1.2×dead load + 1.6×live load) are applied to the test assembly. The magnitude of this load is typically greater than the ASCE 7 load demand for extraordinary events (1.2×dead load + 0.5×live load) since the design of a floor assembly is mostly governed by serviceability, i.e., floor vibration, requiring a deeper beam section. The fire resistance rating of a test assembly is usually determined based on limiting temperatures and displacements as discussed below.

Figure 14 summarizes the test results in comparison with ASTM E119 acceptance criteria. For the 2-hour restrained fire resistance rating, the test specimen must meet a specified combination of the following conditions: (i) sustaining the applied loads with no ignition of cotton waste placed on the top of the heated concrete slab during the full rating period, (ii) the average temperature on unexposed surface less than 139 °C above its initial temperature during the first hour, (iii) a peak temperature of structural steel members below 704 °C during the first hour, and (iv) the average temperature at any section of structural steel members below 593 °C during the first hour, and (v) the maximum total displacement less than the value of $Lc^2/400d$ where Lc = beam clear span, d = depth of composite beam, and the corresponding displacement rate less than the value of $Lc^2/9000d$. As shown in Figure 14, the protected individual W16×31 beams and W18×35 girders of the test assembly successfully met the limiting temperature and displacement criteria. The average concrete surface temperature measured by eight thermocouples distributed across the test assembly was approximately 120 °C prior to extinguishment of the fire. Although the maximum total displacement of the secondary beam exceeded the ASTM E119 displacement limit, the measured displacement rate of this beam was 40 % less than its specified value. It is important to note that this load condition was determined from the ASCE 7 load combination of 1.2×dead load + 0.5×live load, only on the order of 30 % of the load prescribed in the ASTM E119 standard for the same assembly. If the ASTM E119 load was used instead, then the test floor assembly might have achieved the limiting displacement and displacement rate much sooner.

This study revealed some potential issues related to the integrity of a composite floor assembly as part of compartmentation under fire loading. As shown in Figure 15, the center breach in the test floor slab, initiated prior to the specified rating period of 120 min, was accompanied by ruptures of the wire reinforcement in tension at the mid-panel displacement of 350 mm (L/26) or greater. A minimum code-specified amount of the shrinkage reinforcement (60 mm^2/m) used in the test assembly was insufficient to resist thermally induced tension during the investigated fire. Although the exposed steel deck appeared to attain superior ductility at large vertical displacements, failure of side deck joints (screws failure at the decking overlap) and local deck ruptures occurred. Those local failures in the heated decking units allowed the flames and hot gases passing through concrete cracks and above the test compartment. This condition could have potentially ignited cotton waste placed on the unexposed surface, failing to meet the standard fire testing criterion (i) as mentioned above.

6. Summary and Conclusions

This paper presented the results of the first fire experiment on the 9.1 m by 6.1 m composite floor assembly situated on the ground floor in the south middle-edge bay of the two-story steel building, with the structural details commonly used in the current U.S. construction practice. The test floor assembly was subjected to a compartment fire similar to standard fire environments and mechanical loads conforming to the ASCE 7 load combination for extraordinary events (approximately 5 kPa including the assembly self-weight). The fire test conditions as well as a variety of responses of the test assembly to the combined effects of fire and mechanical loading are discussed and compared with the ASTM E119 acceptance criteria.

This test demonstrated that all fire-protected floor beams and girders met the ASTM E119 limiting temperatures. Also, these steel members never reached runaway at large vertical displacements (up to the ratio of L/16). Although the test floor assembly did not collapse during heating, some partial shear ruptures of connecting bolts were discovered during the post-test inspections. However, the heated floor slab exhibited a potential fire hazard before reaching the specified rating period (2 h), because of the use of the minimum code-compliant shrinkage reinforcement of 60 mm^2/m. The test floor slab began to crack along the internal edges of the test column grid less than 30 min after ignition of the fire. The center cracks appeared around the midspan of the secondary beam at 70 min, which rapidly propagated in the east or west direction. The glowing hot deck was finally exposed on the top of the slab through enlarged concrete cracks. This main breach was caused by ruptures of wire reinforcement in tension (due to catenary action) parallel with the deck flutes. The east and west edge cracks which formed within the test column grid resulted in the loss of the east and west vertical supports of the concrete slab over the girders. This initial experiment suggests that the minimum required slab reinforcement currently allowed in the U.S. practice may not be sufficient to maintain the structural integrity of the composite floor assembly during structurally significant fire events.

Further study is recommended to evaluate the potential fire hazard associated with relatively 'thin' slab details permitted in the current construction practice.

More recently, the second fire experiment was conducted to study the influence of enhanced slab design (with an increased area of slab reinforcement), determined based on Choe *et al* (2021b), on the fire performance of composite floor systems, which will be discussed in the authors' future publications.

Acknowledgements

This work was conducted as part of the project "Measurement of Structural Performance in Fire" under the NIST Engineering Laboratory's Fire Risk Reduction in Building Programs. The authors thank William Baker (Skidmore, Owings, and Merrill), Craig Beyler (Jensen Hughes), Luke Bisby (University of Edinburgh), Ian Burgess (University of Sheffield), Charles Carter (AISC), Charles Clifton (University of Auckland), Michael Engelhardt (University of Texas), Graeme Flint (Arup), Nestor Iwankiw (Jensen Hughes), Kevin LaMalva (Warringtonfire), Roberto Leon (Virginia Tech.), and Amit Varma (Purdue University) for their expert consultation. The authors also thank the NIST colleagues including Brian Story, Laurean DeLauter, Anthony Chakalis, Philip Deardorff, Marco Fernandez, Artur Chernovsky, Michael Selepak, Rodney Bryant, Chao Zhang, Jonathan Weigand, Joseph Main, and Fahim Sadek for their significant contributions to design, construction, and execution of this test program.

References

- AISC (American Institute of Steel Construction) (2016). "Specification for Structural Steel Building", *AISC 360-16,* AISC, Chicago, IL.
- ASCE (American Society of Civil Engineers) (2016). "Minimum design loads and associated criteria for buildings and other structures", *ASCE 7-16*, ASCE, Reston, VA.
- ASCE (2018). "Structural Fire Engineering", *ASCE Manual of Practice (MOP) 138,* ASCE, Reston, VA.
- ASTM (American Society of Testing and Materials) (2013). "Standard test method for density, absorption, and voids in hardened concrete", *ASTM C642-13,* ASTM International, West Conshohocken, PA.
- ASTM (2021). "Standard methods of fire test of building construction and materials, ASTM International", *ASTM E119−21,* ASTM International, West Conshohocken, PA.

- Bailey, CG (2003). “Efficient arrangement of reinforcement for membrane behavior of composite floor slabs in fire conditions”, *Journal of Constructional Steel Research*, Vol. 59 No.7, pp 931-949.
- Bisby, L., Gales, J., Maluk, M. (2013). “A contemporary review of large-scale non-standard structural fire testing”, *Fire Science Review*, Vol. 2 No. 1. https://doi.org/10.1186/2193-0414-2-1
- British Steel (1999). “The Behavior of Multi-Story Steel Frame Buildings in Fire”, Rotherham, UK.
- Bryant, R. and Bundy, M. (2019). “The NIST 20 MW calorimetry measurement system for large-fire research”, *Technical Note (NIST TN)–2077*, Gaithersburg, MD. https://doi.org/10.6028/NIST.TN.2077
- Bundy M., Hamins, A., Gross, J., Grosshandler, W., Choe, L. (2016), “Structural fire experimental capabilities at the NIST national fire research laboratory”, *Fire Tech.*, Vol. 52 No. 4, pp. 959-966. https://doi.org/10.1007/s10694-015-0544-4
- Choe, L., Ramesh, S., Grosshandler, et al. (2020). “Composite floor beams with simple shear connections subject to compartment fires: experimental evaluation”, *J. of Str Eng.*, 146, pp. 1-14. https://doi.org/10.1061/(ASCE)ST.1943-541X.0002627
- Choe, L., Ramesh, S., Hoehler, M. (2018). “National fire research laboratory commissioning project: testing steel beams under localized fire exposure”, *Technical Note (NIST TN) – 1983*, p117, Gaithersburg, MD. https://dx.doi.org/10.6028/NIST.TN.1983
- Choe, L., Ramesh, S., Hoehler, M., Seif, M., Bundy, M., Reilly, J., Glisic, B. (2019), Compartment Fire Experiments on Long-Span Composite-Beams with Simple Shear Connections, Part 2: Test Results, Technical Note (NIST TN) – 2055, Gaithersburg, MD, https://10.6028/NIST.TN.2055.
- Choe, L., Ramesh, S. Dai, X. et al. (2021a). “Compartment Fire Experiments on Composite Floor Systems: Background and Test #1”, *Technical Note (NIST TN) – 2165*, Gaithersburg, MD, https://10.6028/NIST.TN.2165.
- Choe, L., Ramesh, S., Zhang, C., Clifton, C. (2021b). “Behaviour of composite floor assemblies subject to fire: Influence of slab reinforcement”, *Proc. of 2021 Eurosteel Conference*, September 1-3, 2021, University of Sheffield, United Kingdom (in production
- Dai, X., Choe, L., Fischer, E., Clifton, C. (2020). “Thermal response and capacity of beam and shear connections during a large compartment fire experiment”, *Proc. of the*

11th International Conference on Structures in Fire (SiF' 20), November 30 – December 02, 2020, University of Queensland, Australia

- ISO (International Organization for Standardization) (2019), "Fire-Resistance Tests – Elements of Building Construction", *ISO 834-2:2019*, Geneva. Available at https://www.iso.org/standard/75137.html
- Maluk, C., Bisby, L., Terrasi, G.P. (2017). "Effects of polypropylene fibre type and dose on the propensity for heat-induced concrete spalling", *Eng. Struct.*, 141, pp. 584–595. https://doi.org/10.1016/j.engstruct.2017.03.058
- Ramesh, S., Choe, L., Seif, M., et al. (2019). "Compartment fire experiments on long-span composite beams with simple shear connections Part 1: experimental design and beam behavior at ambient temperature", *Technical Note (NIST TN) - 2054*, p141, Gaithersburg, MD. https://dx.doi.org/10.6028/NIST.TN.2054
- SDI (Steel Deck Institute), *C-2017 Standard for composite steel floor deck-slabs*, SDI. http://www.sdi.org/wp-content/uploads/2017/02/ANSI-SDI-C-2017-Standard.pdf
- Taylor B. and Kuyatt, C. (1994). "Guidelines for Evaluating and Expressing the Uncertainty of NIST Measurement Results", *Technical Note (NIST TN) – 1297*, p24, Gaithersburg, MD. https://doi.org/10.6028/NIST.TN.1297
- Vassart, O., Zhao, B., Hamerlink R., Hauke, B. et al (2014). "Membrane action in fire design of composite slab with solid and cellular steel beams – valorisation (MACS+)", *EUR 26682*, European Commission, Luxembourg.
- Wald. F., Simoes da Silva, L., Moore, D., Lennon, T., Chaldna, M., Santiago, M., Benes, M., Borges, L. (2006). "Experimental behaviour of a steel structure under natural fire", *Fire Safety Journal,* Vol. 41 No. 7, pp.509–522.
- Zhang, C., Grosshandler W., Sauca A., and Choe L. (2019). "Design of an ASTM E119 fire environment in a large compartment", *Fire Tech.*, pp. 1–23.
- Zhao, B., Roosefid, M., Vassart, O. (2008). "Full scale test of a steel and concrete composite floor exposed to ISO fire and corresponding numerical investigation", paper presented at Eurosteel Conference, 3-5 Sep, Graz, Austria.
- Zhao, B. and Roosefid, M. (2011). "Experimental and numerical investigations of steel and concrete composite floors subjected to ISO fire condition," *Journal of Structural Fire Engineering*, Vol. 2 No. 4, pp.301-310.

Table 1 - Key features of previous fire experiments on full-scale composite floor systems

Reference	Test Name	Fire compartment	Test fire	Approx. Mechanical load	Min. concrete thickness above profiled steel decking	Steel mesh
British Steel (1999)	Test 3	Corner bay 10 m x 7.6 m (Floor) 6.6 m x 1.8 m (Opening)	Wood cribs (45 kg/m^2)	5.5 kN/m^2	70 mm (130 mm)	142 mm^2/m
British Steel (1999)	Test 4	Corner bay 9 m x 6 m (Floor)	Wood cribs (40 kg/m^2)	5.5 kN/m^2	70 mm (130 mm)	142 mm^2/m
Wald et al. (2006)	Test 7	Edge bay 11 m x 7 m (Floor) 9 m x 1.3 m (Opening)	Wood cribs (40 kg/m^2)	6 kN/m^2	70 mm (130 mm)	142 mm^2/m
Zhao et al. (2008)	FRACOF	Furnace 8.7 m x 6.7 m (Floor)	ISO 834 (2 hr)	5 kN/m^2	97 mm (155 mm)	256 mm^2/m
Zhao and Roosfid (2011)	COSSFIRE	Furnace 9 m by 6.7 m (Floor)	ISO 834 (2 hr)	4 kN/m^2	77 mm (135 mm)	256 mm^2/m

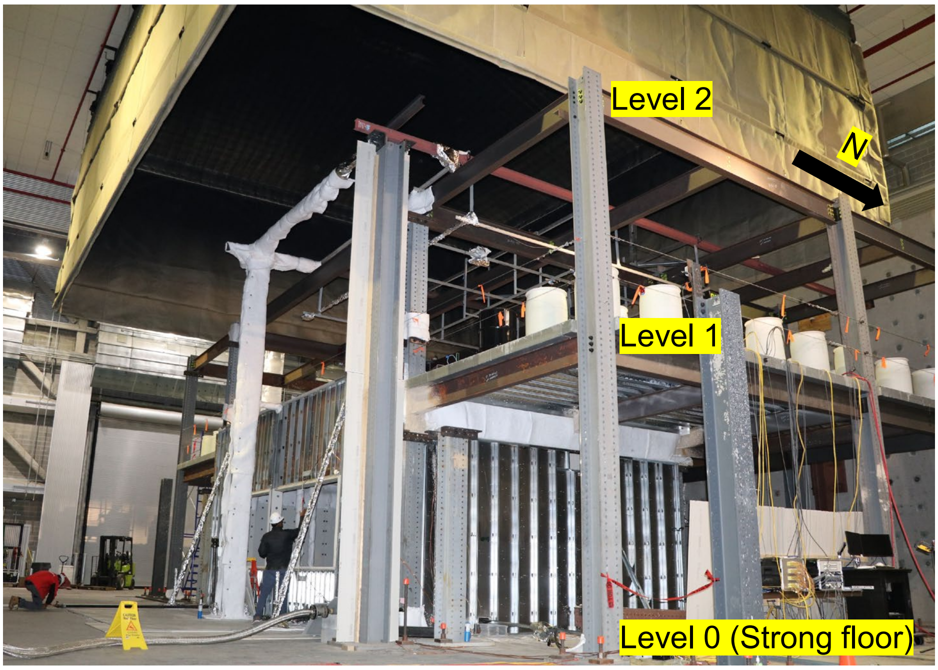

Figure 1- Two-story test building at the NFRL

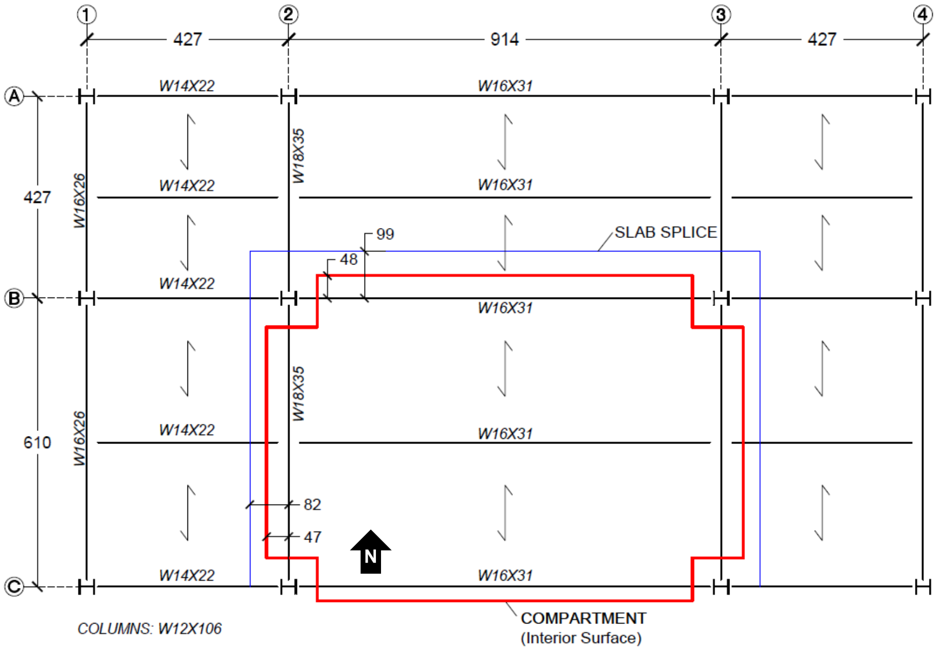

Figure 2- Building floor plan (dimensions in cm)

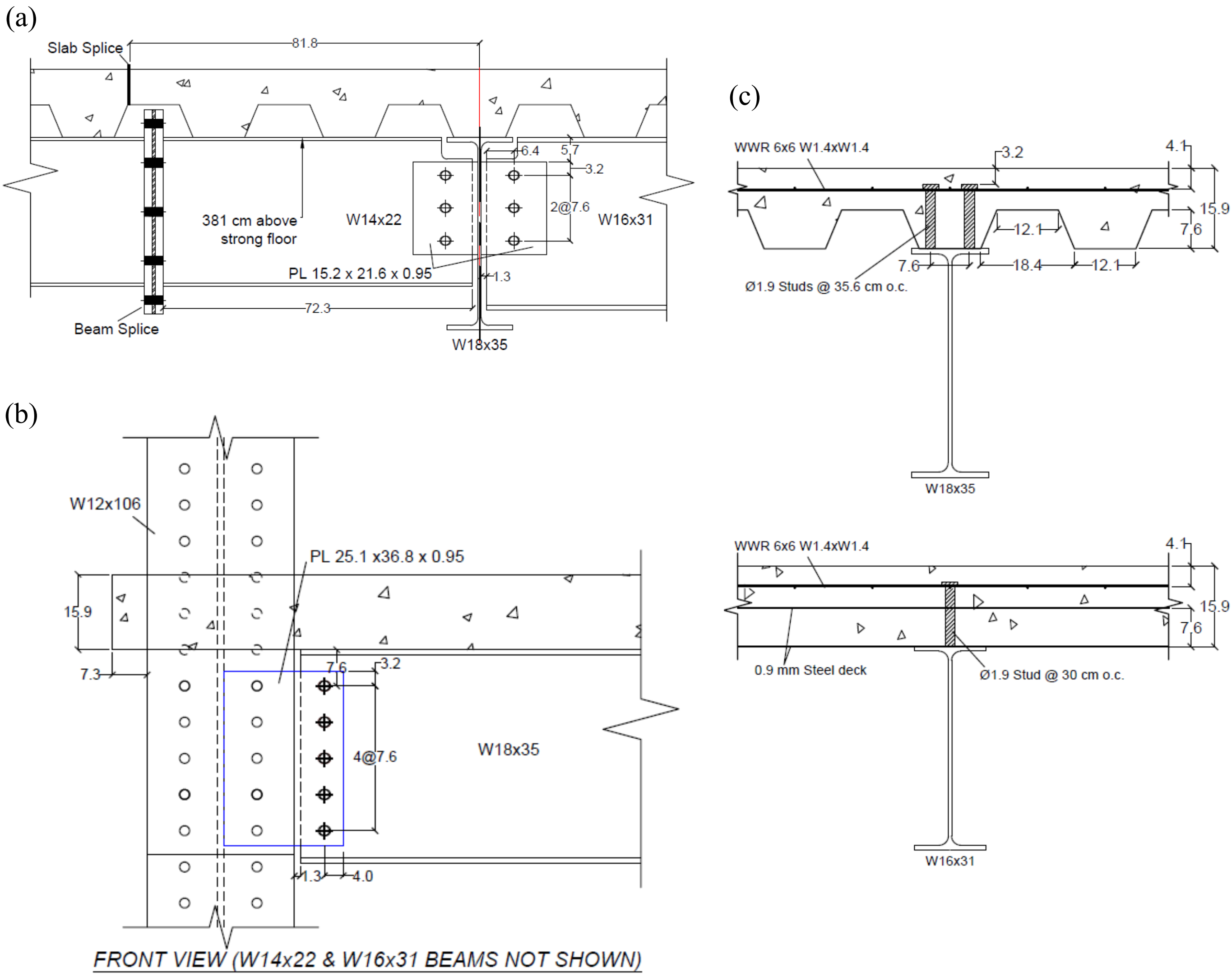

Figure 3 – Floor frame details: (a) standard shear tab; (b) extended shear tab; (c) composite beam sections (dimensions in cm; structural W-shapes in U.S. customary units)

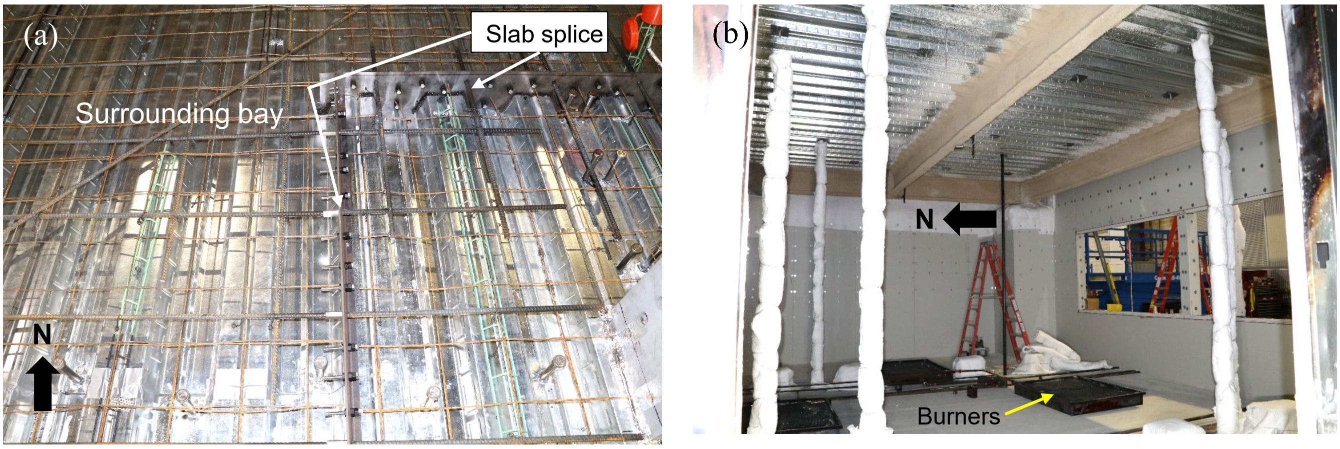

Figure 4 – Pre-test photographs : (a) steel reinforcement details of slab splices; (b) fire test compartment with the main opening on the south wall

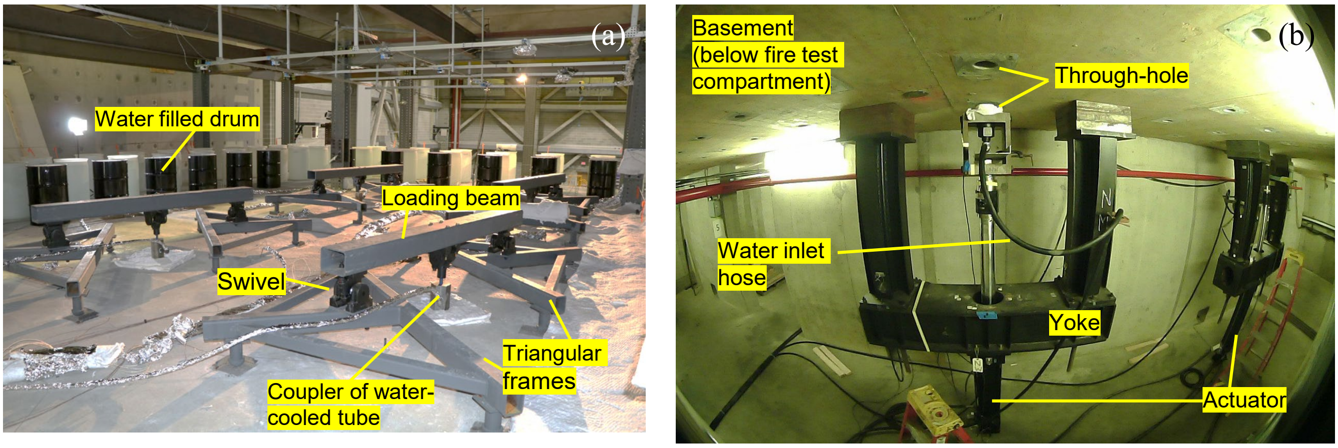

Figure 5 – Pre-test photographs: (a) loading frame above the test floor assembly; (b) servo-hydraulic actuators with water-cooled tubes (tubes not shown in photo)

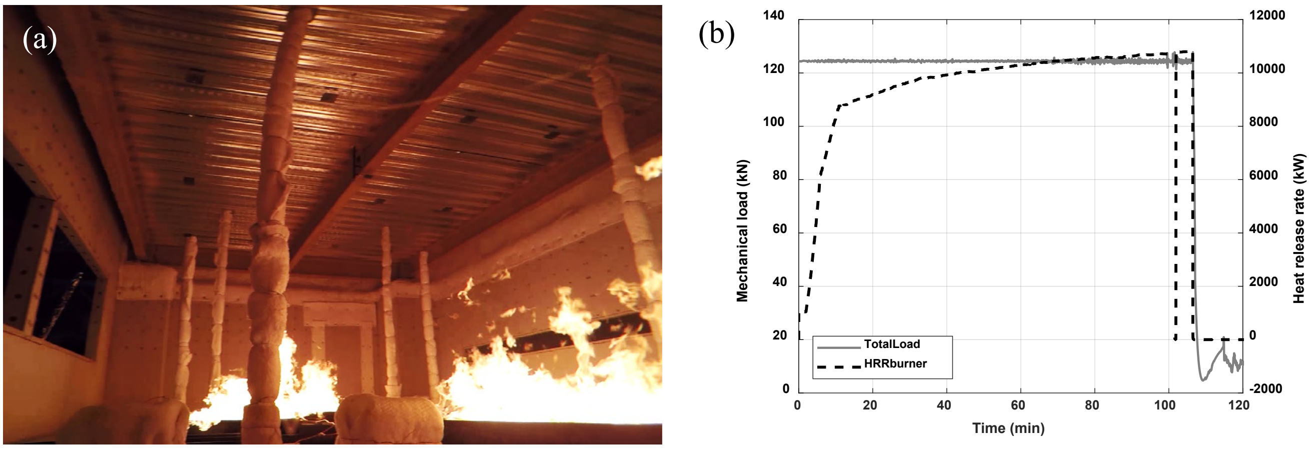

Figure 6 – (a) Snapshot from video taken inside the fire test compartment 3 min after ignition; (b) time history of total actuator mechanical load (TotalLoad) and heat release rate of burners (HRRburner)

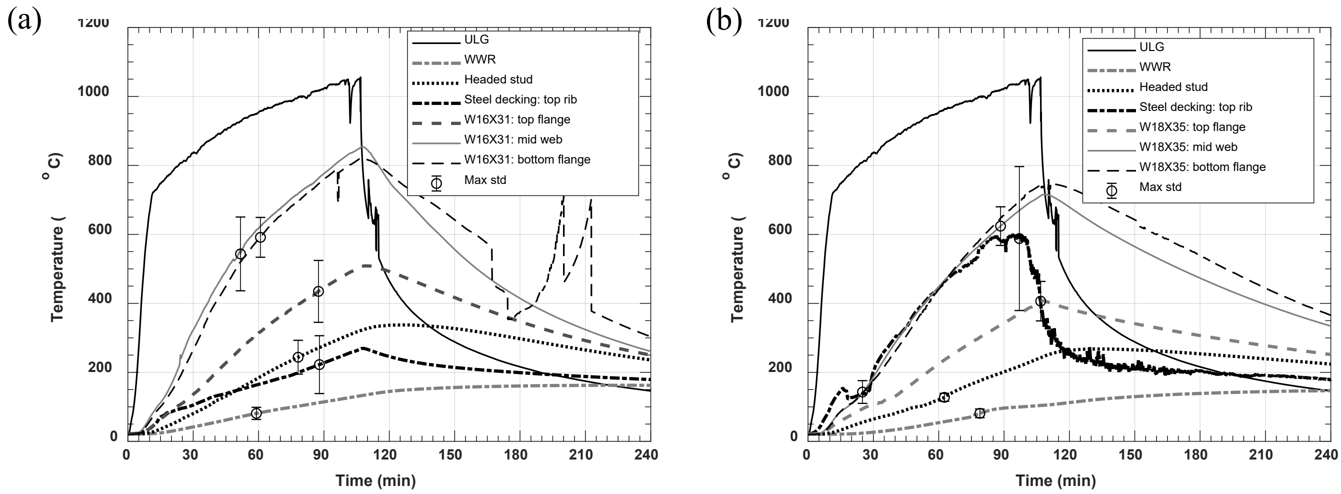

Figure 7 – (a) Measured temperatures of W16×31 composite beam and (b) W18×35 composite girder. Plotted with average values of three W16×31 beams and W18×35 girders within the test compartment

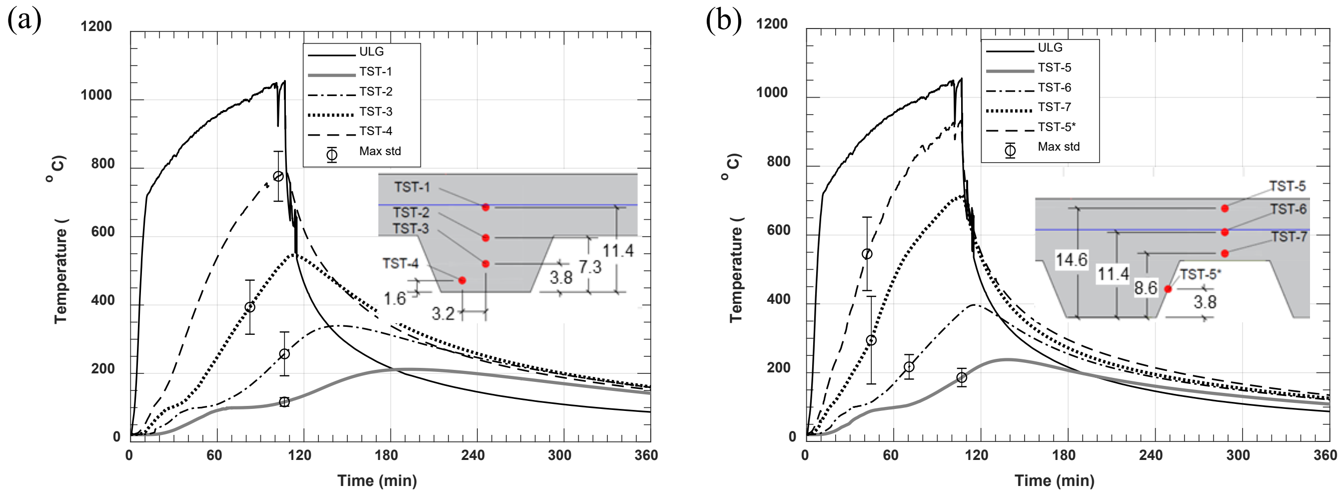

Figure 8 – Measured temperatures of (a) deep section and (b) shallow section of the concrete floor slab. Plotted with the average values of six deep sections or four shallow sections across the test floor; thermocouple locations are in cm

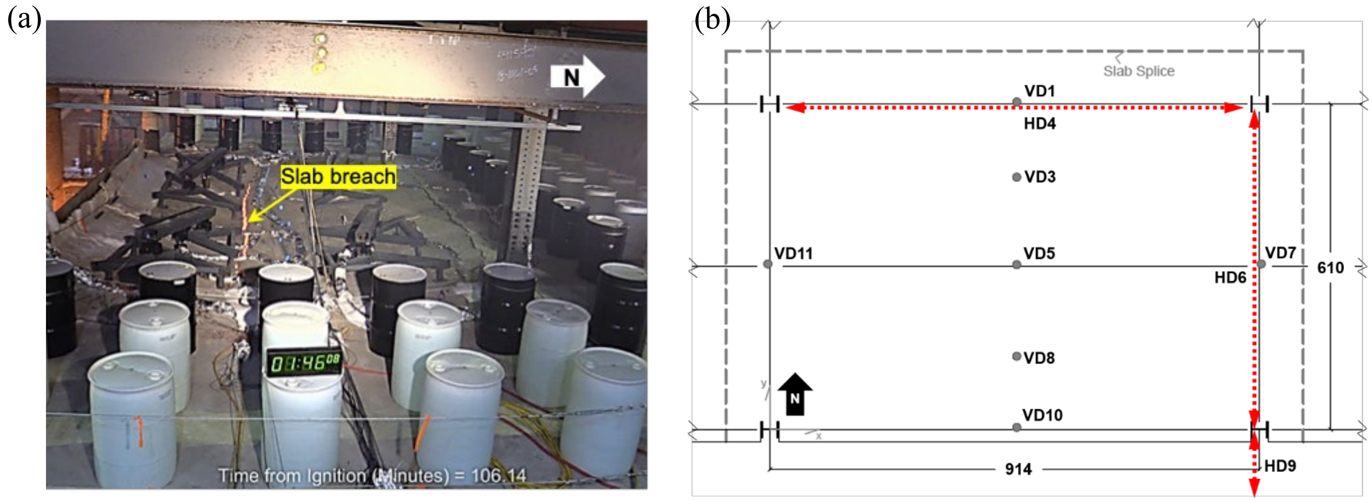

Figure 9 – (a) Breach of the test floor slab; (b) Locations of displacement measurements with dimensions in cm

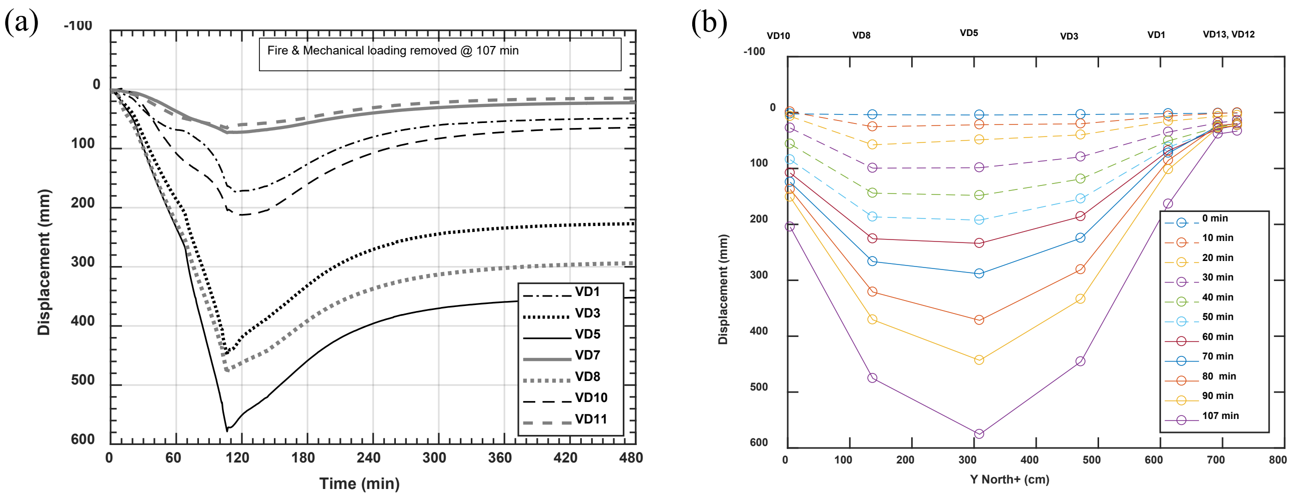

Figure 10 – (a) Vertical displacements after the burner ignition at 0 min; (b) Vertical displacement profile varying with fire exposure time

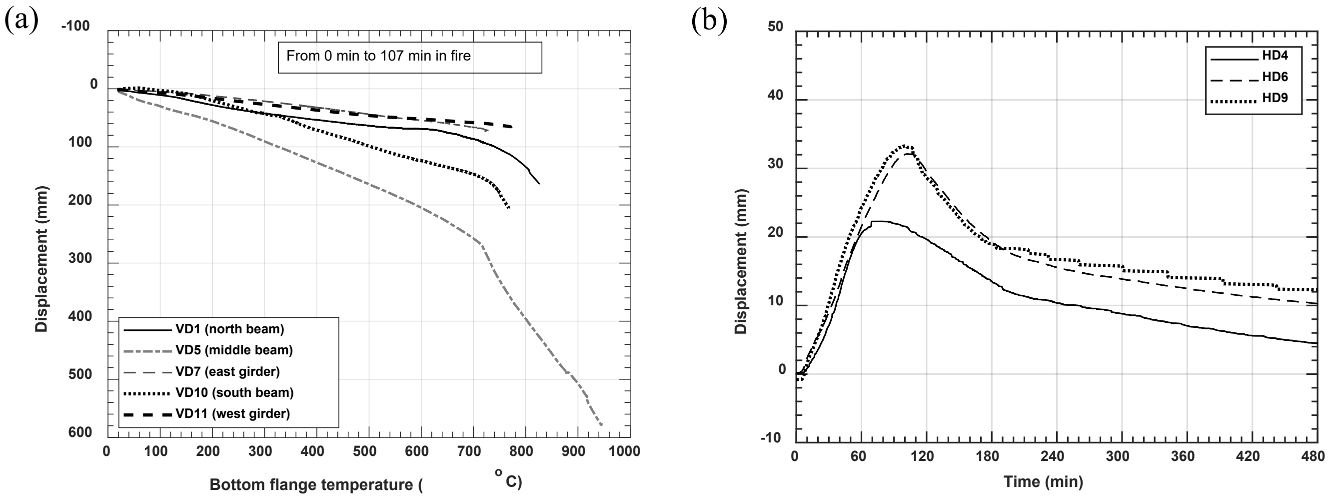

Figure 11 – (a) Vertical displacement data as a function of bottom flange temperatures during heating; (b) Horizonal displacements measured at 15 cm above the test floor slab during heating (until 107 min) and cooling

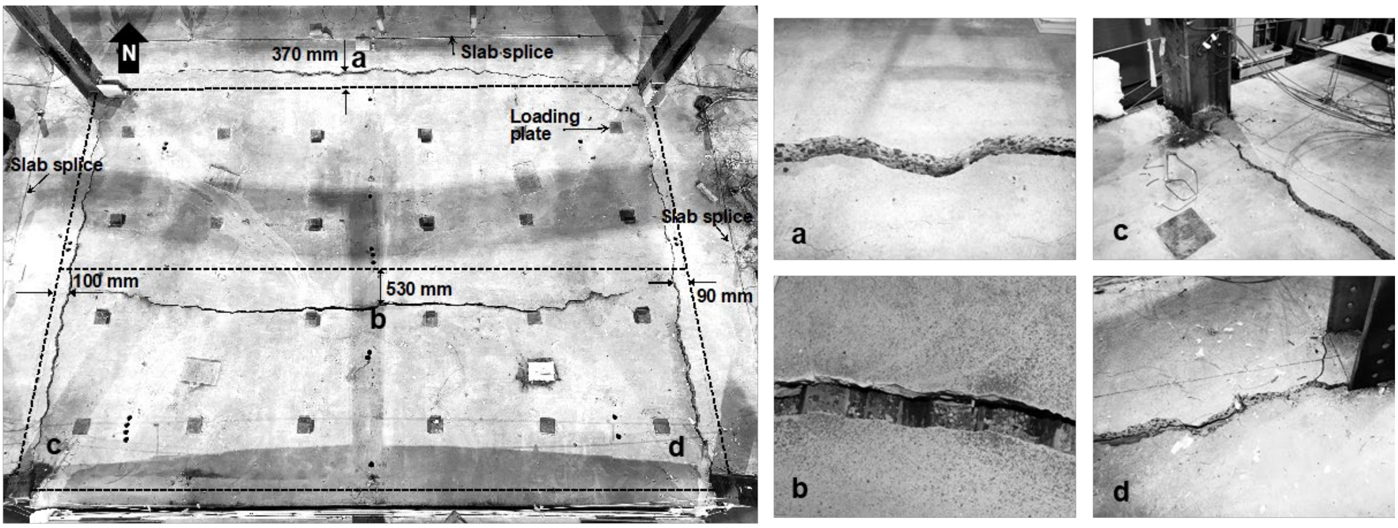

Figure 12 – Top of the test floor slab after cooling. Dashed lines define the test-bay column grid. The four photographs on the right (a through d) show close-ups of concrete fractures

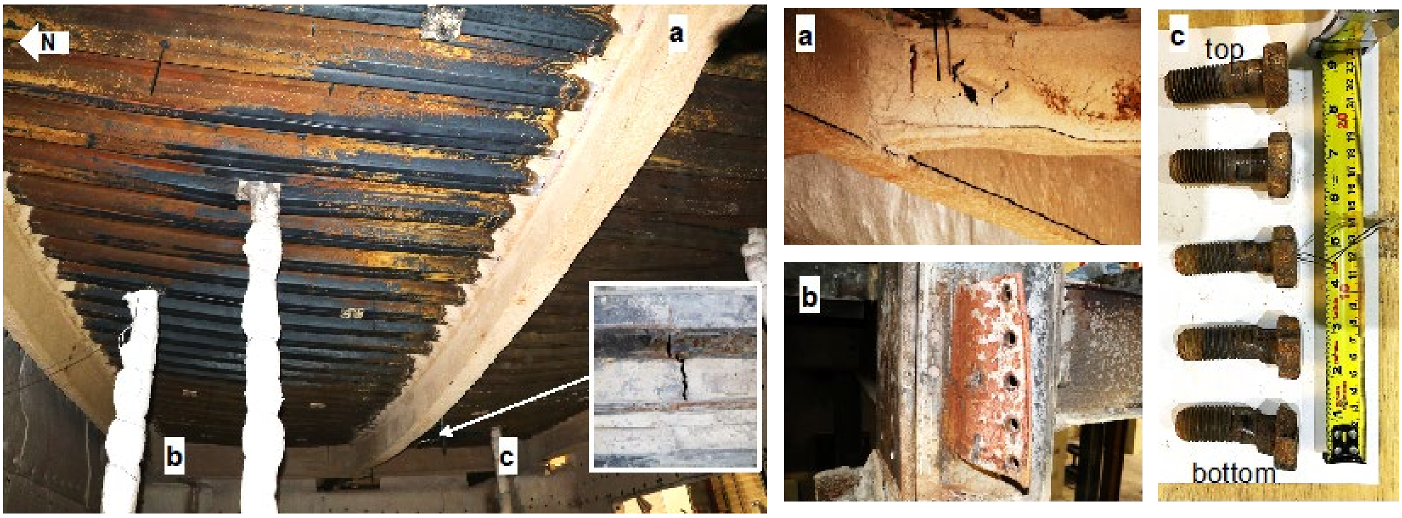

Figure 13 – Fire-exposed steelwork of the test floor assembly after cooling. Close-ups of some deflected steel parts are shown in images a through c

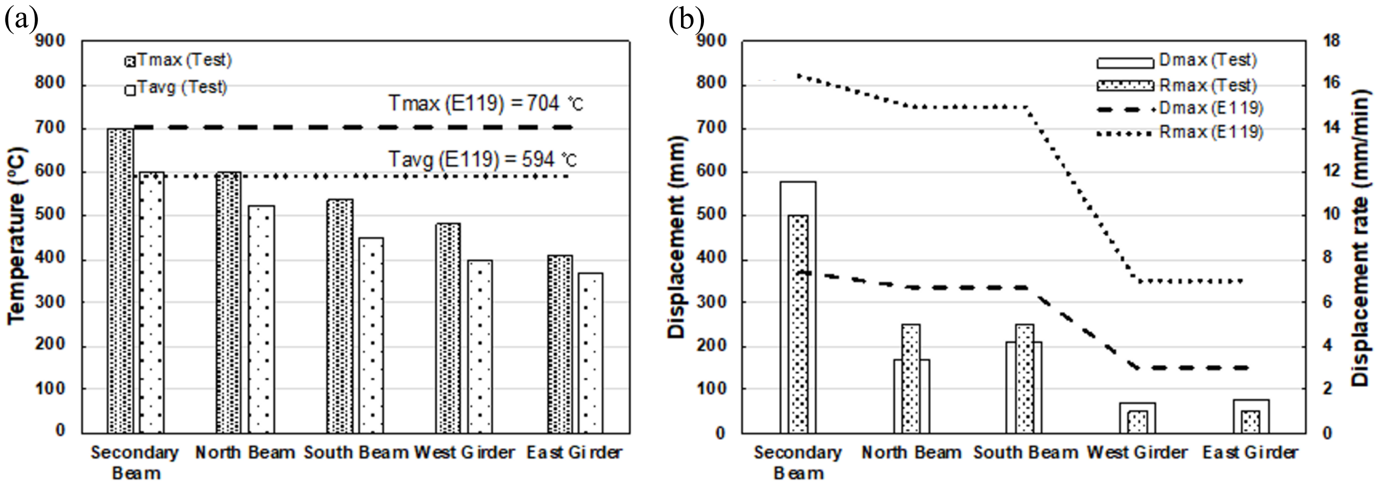

Figure 14 – Comparisons of the test results with (a) limiting temperatures and (b) limiting displacements and displacement rates, where Dmax = maximum displacement and Rmax = maximum displacement rate

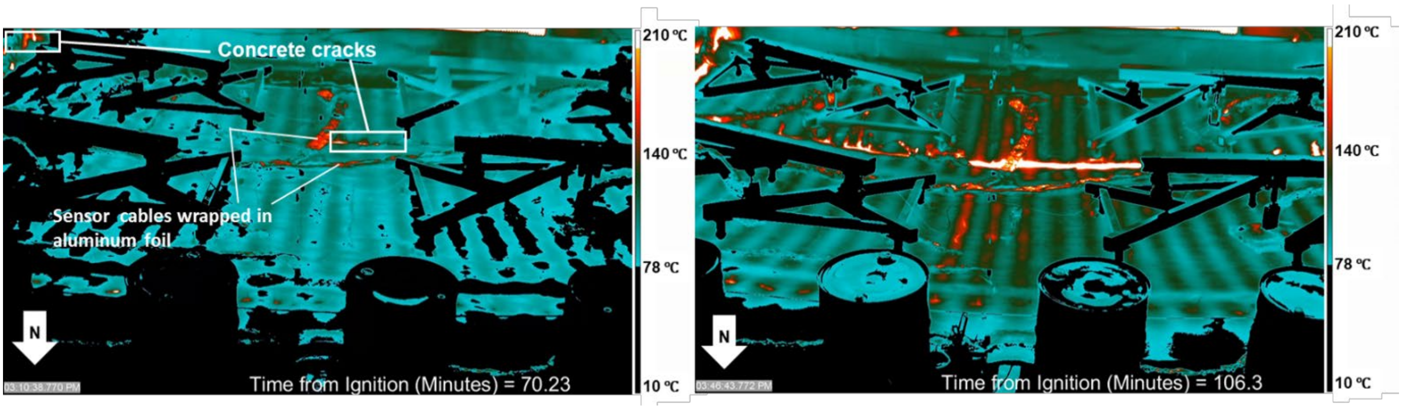

Figure 15 – Thermal images of the top of the test floor slab at 70 min and 106 min after fire ignition